

Marijonas BOGDEVICIUS
Rasa ZYGIENE

RESEARCH OF DYNAMIC PROCESSES OF THE SYSTEM "VEHICLE – TRACK" USING THE NEW METHOD OF VEHICLE WHEEL WITH METAL SCALE

BADANIE DYNAMICZNYCH PROCESÓW ZACHODZĄCYCH W UKŁADZIE „POJAZD-TOR” Z WYKORZYSTANIEM NOWEJ METODY DLA KÓŁ Z METALOWĄ ŁUSKĄ

Mathematical models of vehicle wheel with metal scales are introduced in this article. When analysing the interaction between vehicle wheel with a metal scale and rail in the system "Vehicle – Track", the changes of the kinematic and dynamic parameters of the wheel and rail contact points in time are examined, depending on the height of the 2 mm metal scale, when the length of the metal scale is 100 mm and the speed of movement is $V = 40 - 100$ km/h. The results obtained after the research of the system "Vehicle – Track", when the wheel has a metal scale, help to better understand and evaluate the impact of metal scale on wheel on dynamic loads of rail and vehicle and the regularities of their movement. The appearance of a metal scale on the wheel's surface causes technical and maintenances problems for the rolling stock. Railway standards limit the speed of movement that depends on a certain size of metal scale.

Keywords: rail-wheel interaction; spatial model of metal scale; contact area; impact force; friction force; vibration.

W niniejszym artykule przedstawiono modele matematyczne koła pojazdu szynowego z powstałą w wyniku zużycia metalową łuską. Analizując oddziaływania pomiędzy kołem pojazdu z łuską a szyną w układzie "pojazd-tor", badano zmiany kinematycznych i dynamicznych parametrów punktów kontaktu koła z szyną zachodzące w czasie, w zależności od wysokości metalowej łuski (2 mm), przy długości łuski 100 mm i zakresie prędkości ruchu pojazdu $V = 40-100$ km/h. Wyniki uzyskane w badaniu układu "pojazd-tor" dla kół na powierzchni których powstała metalowa łuska, umożliwiają lepsze zrozumienie oraz ocenę wpływu łuski na dynamiczne obciążenia szyny i pojazdu oraz prawidłowości ruchu pojazdu. Pojawienie się metalowej łuski na powierzchni koła powoduje problemy techniczne i obsługowe w utrzymaniu ruchu taboru kolejowego. Normy kolejowe ograniczają prędkość ruchu pojazdów szynowych, uzależniając ją od rozmiaru łuski.

Słowa kluczowe: oddziaływania koło–szyna; przestrzenny model łuski metalowej; obszar kontaktu; siła uderzenia; siła tarcia; wibracja.

1. Introduction

The precise operation of modern machines and vehicles can only be ensured by complex measures, which consist of modern construction solutions for design, the use of high-quality and suitable operational and structural materials, and quality maintenance, which is done on time.

Multicriteria decision-making is widely used in all areas. Multicriteria assessment models are presented in the field of transport [24, 27]. Using the [20] multicriterion additive model, it was found that the main parameter of the technical condition of the railway track is the speed of the wagon.

Initial surface of vehicle wheel profile is symmetric. The radius of vehicle wheel is equal at all points. However, during exploitation, roughness appears on the surfaces of wheel and rail profiles, due to interaction between vehicle wheel and rail, and their different geometrical surfaces. Furthermore, the wheel profile constantly changes and becomes asymmetrical.

Damages on surfaces of wheel and rail mostly appear due to their interaction. However, they may also occur due to various manufacturing inaccuracies and poor quality of machined parts. Wheel and rail damages are rarely found on initial stages of exploitation, and over time, the damages increase and may cause irreversible consequences.

To reduce the risk of train accidents, railway traffic risk management models are being developed [6], which enable railway managers to improve their traffic safety strategy by determining the priorities of the required measures.

Most of the vehicle wheel damage occurs due to braking, surface roughness, temperature differences, and other factors. Metal plasticity methods are used to evaluate the mechanical condition (determine strength and plasticity characteristics) of solid moulding wheels of the wagon [28]. The theoretical angular speeds of the loaded wheels are different due to disproportionate loads and although they are forced to move at the same speed as the wagon, the wheels are sometimes forced to tow and even slip unevenly.

The most common damage in wheel is flat, which occurs due to wheel slip or stuck brake pads [31]. Increase in wheel damages has been examined in the article [10].

Metal scales on wheel occur due to thermomechanical damages. Intensive plastic metal deformation appears due to sudden braking, short-term wheel skidding and jumping, when the metal of the wheel suddenly heats up and then suddenly cools down. Sudden braking means the braking of the train in exceptional cases, in these circumstances the largest braking force is used when the air is released from the brake pipe [26].

Many metal scales can appear on the rolling surface of the wheel, which can have one or more layers and differ in height. U-shaped scales are the most common to occur. The damages of scaled wheel are measured from the surface intact to the highest point of the scale. During the exploitation, the metal scale can become even more layered and can even come off the wheel surface. The hardness of metal scale is about 900 HV, which is typical for tempered steel with high residual stress.

In the case of scaled wheel, large impact forces appear in the contact between the wheel and rail, which load the rail and wheelset bearings. Wheel flats frequently appear on the rolling surface of the wheel due to metal scales.

The metal scale on wheel may form when the wheel is broken extremely. Due to large frictional forces and increased temperatures, the metal on the wheel melts and a certain layer of metal is cut off. A flat develops in the contact zone, and the molten metal flows outside the contact zone and to the surface of the wheelset. If the wheel continues to rotate, the moulded metal cools off and continues to deform when it comes in the contact with the rail. This is how the multi-layered metal scale forms on the surface of wheel (Fig. 1, Fig. 2).

Railway vehicle exploitation in Lithuanian Railways (JSC Lithuanian Railways) [22] is prohibited, when wheel has a scale with height higher than 0.5 mm in passenger cars and 1 mm in freight cars.

The authors [2-5, 27] usually choose flat as vehicle wheel damage to simplify the mathematical models, as it is the most common damage in vehicle wheel.

The contact zone of wheel and rail is described as a point and the geometry of the wheel as an analytical function in the mathematical models of interaction between wheel and rail [1, 15, 17, 18, 19, 20, 21, 22, 23].

Researchers [9, 16, 29, 30] describe variations of mass accelerations and displacements of wagon and rail in time or path length, in their studies of dynamical processes that occur in the interaction between wheel and rail. It was determined that the maximum acceleration value is obtained in the case of a wheel with a flat.

Parameters of the deformation of the isolated sinusoidal shape and the influence of the wagon speed on the vertical vibration of the body are evaluated in the dynamic models of interaction between the vehicle and track [12].

The influence of contact forces on the deformation of rolling carload wheels and rails, and the influence of this deformation on the redistribution of the contact stresses is also investigated [25].

Theoretical and practical study of the surface roughness of interaction between rail and train defined the values the surface roughness, when interacting with different rail profiles that affect the increase in exploitation time [11].

Research has been carried out [8] to improve the safe operation of trains and increase the efficiency of load assessments.

Rail condition is assessed [7,13,14] by using the movements of axle-box and bodies, estimating and analysing accelerations.

The authors of this article have failed to find other researches about metal scale in wheelset wheel.

The article consists of three chapters. In the first chapter the system „Vehicle – Track” and literature relevant to its elements are analysed. In the second chapter authors present a mathematical model of wheelset wheel with a metal scale and briefly describe the model of system „Vehicle – Track” and present a calculation algorithm for this system. The third chapter consists of the results of the calculations and discussion.

This paper presents mathematical models of a vehicle wheel with a 2 mm metal scale. The mathematical model allows examination of the interaction between wheel with a metal scale and the rail and displays its effect on dynamic loads. The new mathematical model allows evaluation of the rotation of the wheel around its longitudinal axis Y, in order to evaluate the rotation of the wheel and determine its slip on the rails. In this article, the authors seek to determine the slip of

the wheel with a defect, when the defect is a metal scale and without a wheel defect. In the case of sliding the wheel in relation to the rail, frictional forces occur, and heat is released, which increases the wheel and rail temperature in the contact area.

The paper shows results of the changes in kinematic parameters of a wheel (angular velocity and acceleration, velocities, accelerations and other parameters) and dynamic parameters (forces and other parameters), depending on the geometry of metal wheel scale, movement speed and other parameters of the system “Vehicle – Track”.

2. Materials and Methods

2.1. The scope of calculations and numerical characteristics of an adhesive joint

During exploitation, the metal scale on wheel can take on various forms. Therefore, this article presents a method for shape generation of metal scale of a wheel and allows generation of a wheel profile with a metal scale if the exact geometry is known.

The mathematical model created in respect to the geometry of metal scale shown in Figure 1 is described in this section. The metal scale of wheelset wheel that consists of three layers is shown in Figure 1 (real top view), where N_{layer} are the layers of metal scale.

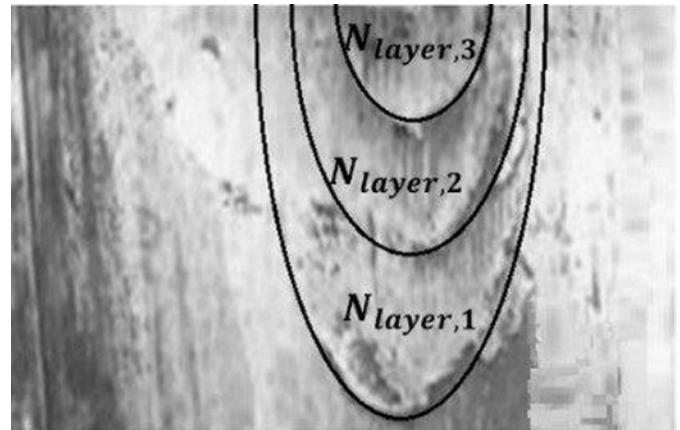


Fig. 1. The metal scale of wheelset wheel, that consists of three layers (real top view)

Metal scales are rarely included in the calculations of mathematical models of railway system “Vehicle – Track”, due to complex and different geometrical shapes (Fig. 2). There are only a few known scientific articles about wheel damage, called metal scale, and its effects on the system “Vehicle – Track”.



Fig. 2. Multi-layered metal scale of wheelset wheel

The developed mathematical model allows generating more metal scales on wheel and more layers of the metal scale (Fig. 2).

The geometry of the wheel and the metal scale on it is shown in Figure 3.

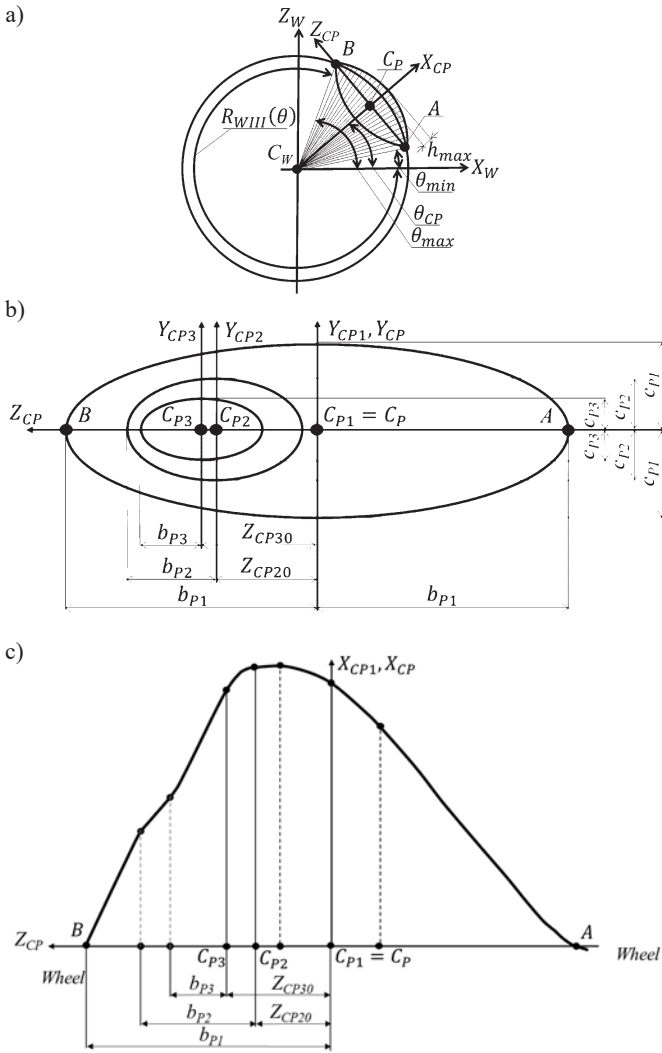


Fig. 3. Computational scheme of metal scale of wheel: a) wheel profile; b) geometrical parameters of metal scale of wheel in directions Y_{CP} and Z_{CP} ; c) geometrical parameters of metal scale of wheel in directions X_{CP} and Z_{CP}

The width of the i -th layer of wheel metal scale is $2c_{P_i}$, and the length is $2b_{P_i}$. Maximum length of metal scale is $2b_{P_1}$. Points A and B (Fig. 3) indicate the start and end of metal scale of vehicle wheels. The geometry of metal scale is described in local coordinate system X_{CP}, Y_{CP}, Z_{CP} . Points $C_{P_1}, C_{P_2}, C_{P_3}$ are the centre points of the metal scale layers. Z_{CP20}, Z_{CP30} (Fig. 3a and Fig. 3b) are the coordinates of centre points Z_{CP} of second and third layers, furthermore $Z_{CP10} = 0$.

The maximum height of metal scale h_{max} (Fig. 3a) is equal to the difference between maximum wheel radius R_{W1} and nominal wheel radius R_W . The size of angles θ_{max} and θ_{min} (Fig. 3a) depends on the position of scale on the surface of the wheel and indicates the maximum and minimum angle size, when generating wheel profile with a metal scale. The position of the scale centre C_P can be described as centre angle $\theta_{CP} = \frac{(\theta_{max} + \theta_{min})}{2}$.

When developing the geometrical model of metal scale of vehicle wheel it is accepted that:

- The metal scale of the vehicle wheel consists of N_{layer} layers (Fig. 1).
- The profile of metal scale is generated in local coordinate system X_{CP}, Y_{CP}, Z_{CP} .
- Each centre of metal scale layer can be moved in Z_{CP} axis by a value of Z_{CPi0} , but $Z_{CP10} = 0$.
- Geometrical parameters of each metal scale layer (starting from the second layer) are independent values that are selected in such way, that total profile of metal scales would be generated as accurate as possible.

It is assumed, that metal scale of vehicle wheel is between points A and B , when the centre angle θ (Fig. 3a) varies from θ_{min} to θ_{max} , i.e. $\theta \in [\theta_{min}, \theta_{max}]$. The section between points A and B is divided to $N_P - 1$ intervals, where N_P – total number of points on the surface of generated scale.

During interpretation of the geometry of a metal scale, it is assumed that the number of layers of the calculated metal sheet is $N_{layer} = 3$ (Fig.1, Fig. 3 b, c).

When generating a wheel profile with one scale, the perimeter of the vehicle wheel surface is divided into three: I zone, when $0 \leq \theta < \theta_{min}$; II zone, when $\theta_{min} \leq \theta < \theta_{max}$; III zone, when $\theta_{max} \leq \theta < 2\pi$.

A change of radius in vehicle wheel with metal scale is described as a function $R_{WII}(\theta)$ in the second zone. Changes of radius in the first and the third zones of vehicle wheel with metal scale can be approximated in the same way as in the second zone, when the weariness of vehicle wheel is known in each of the zones.

By knowing the variation of vehicle wheel radius R_W in each zone, it is possible write the function $R_W(\theta)$ of changes in vehicle wheel radius, over the whole perimeter of the wheel surface:

$$R_W(\theta) = R_{WI}(\theta)[H(\theta) - H(\theta - \theta_{min})] + R_{WII}(\theta) + R_{WIII}(\theta)[H(\theta - \theta_{max}) - H(\theta - 2\pi)] \quad (2)$$

where $R_{WI}(\theta), R_{WIII}(\theta)$ are known wheel radius functions in the first and third zones, $R_{WII}(\theta)$ is the radius function in the second zone (Fig. 3 a), H is Heaviside step function.

Wheel radius function $H R_{WII}(\theta)$ in the second zone is:

$$R_{WII}(\theta) = \sum_{i=1}^{N_P-1} R_{W,i,i+1}(\theta)[H(\theta - \theta_i) - H(\theta - \theta_{i+1})], \quad (3)$$

where $R_{W,i,i+1}(\theta)$ is radius function between points i and $i + 1$,

$$R_{W,i,i+1}(\theta) = N_1(\xi)R_W(\theta_i) + N_2(\xi)R_W\left(\frac{(\theta_i + \theta_{i+1})}{2}\right) + N_3(\xi)R_W(\theta_{i+1}) \quad (4)$$

where ξ dimensionless coordinate, $N_j(\xi)$ is shape function, $j = 1, 2, 3$.

Dimensionless coordinate ξ is:

$$\xi = \frac{(\theta - \theta_i)}{\theta_{i+1} - \theta_i}, \text{ when } \xi \in [0, 1]. \quad (5)$$

The shape functions $N_j(\xi)$ are equal:

$$N_1(\xi) = (2\xi - 1)(\xi - 1), N_2(\xi) = 4\xi(1 - \xi), N_3(\xi) = \xi(2\xi - 1). \quad (6)$$

In the coordinate system X_{CP} , Y_{CP} in Z_{CP} (Fig. 3c) the total scale profile consists of multiple profiles of scale layers. The k -th profile of scale layer is described as a function:

$$\left(\frac{Z_{CP} - Z_{CPk0}}{b_{Pk}}\right)^{n_{ZPk}} + \left(\frac{X_{CP}}{a_{Pk}}\right)^{n_{XPk}} + \left(\frac{Y_{CP} - Y_{CPk0}}{c_{Pk}}\right)^{n_{YPk}} = 1, \quad (7)$$

where n_{XPk} , n_{YPk} , n_{ZPk} are known exponents, a_{Pk} , b_{Pk} , c_{Pk} are halves of the layer length (Fig. 3 b), Z_{CPk0} and Y_{CPk0} is the k -th layer centre coordinate of metal scale.

The height of k -th metal scale layer of vehicle wheel is:

$$X_{CPk} = a_{Pk} \left[1 - \left(\frac{Z_{CP} - Z_{CPk0}}{b_{Pk}}\right)^{n_{ZPk}} - \left(\frac{Y_{CP} - Y_{CPk0}}{c_{Pk}}\right)^{n_{YPk}} \right]^{n_{XPk}} \quad (8)$$

After adding the entire metal scale layer functions X_{CPk} general scale profile function is generated:

$$f_{P0}(Z_{CP}) = \sum_{k=1}^{N_{layer}} a_{Pk} \left[1 - \left(\frac{Z_{CP} - Z_{CPk0}}{b_{Pk}}\right)^{n_{ZPk}} \right]^{n_{XPk}} \cdot [H(Y_{CP} + c_{Pk}) - H(Y_{CP} - c_{Pk})] \cdot H[(Z_{CP} + b_{Pk}) - H(Z_{CP} - b_{Pk})] - \sqrt{R_W^2 - Z_{CP}^2 - R_{WCP}^2}, \quad (9)$$

where R_W is nominal wheel radius, R_{WCP} is wheel radius from wheel centre C_W to point C_P (Fig. 3),

$$R_{WCP} = \sqrt{R_W^2 - b_{P1}^2}, \text{ when } -b_{P1} \leq Z_{CP} \leq b_{P1} \quad (10)$$

Usually, the metal scale on the vehicle wheel has a smooth surface (Fig. 1), therefore, the generated scale function (9) is approximated in the following way:

$$f_P(Y_{CP}, Z_{CP}) = f_{P0}(Y_{CP}, Z_{CP}) \Phi(Y_{CP}, Z_{CP}). \quad (11)$$

where $\Phi(Y_{CP}, Z_{CP})$ is one of the possible metal scale alignment functions:

$$\Phi(Y_{CP}, Z_{CP}) = \left(\cos\left(\frac{\pi Z_{CP}}{2b_{Pk}}\right) \right)^{nzc} \left(\cos\left(\frac{\pi Y_{CP}}{2c_{Pk}}\right) \right)^{nyc}, \quad (12)$$

where nzc and nyc are exponents.

General function of metal scale profile is described:

$$f_P(Z_{CP}) = \sum_{k=1}^{N_{layer}} a_{Pk} \left[1 - \left(\frac{Z_{CP} - Z_{CPk0}}{b_{Pk}}\right)^{n_{ZPk}} \right] \left[H(Z_{CP} + b_{Pk}) - H(Z_{CP} - b_{Pk}) \right] - \sqrt{R_W^2 - Z_{CP}^2} - \sqrt{R_W^2 - b_{P1}^2}. \quad (13)$$

General metal scale function $f_P(Z_{CP})$ Equation (13) is used during examination of the metal scale profile X_{CP} in Z_{CP} direction, in further calculations.

2.2. Mathematical model of system "Vehicle – Track", when the vehicle wheel is scaled

The previously created mathematical model [5, 27] of "Vehicle – Track" (Fig. 4) has been used for most of calculations, which is com-

posed of several mathematical models and designed to determine the forces acting during the interaction between rail and damaged wheel.

This mathematical model assesses the speed of the vehicle, the geometric parameters of the interacting bodies, their physical and mechanical properties, and allows determination of the changes in the forces acting during contact.

The mathematical model of the system "Vehicle – Track" for wheel with a metal scale is used on two-dimensional space. It is assumed that $Y = 0$.

Many parameters that appear in the contact zone of wheel and rail, between two contacting surface points and at every time moment can be determined by using this mathematical model [5, 27]: wheel slip, friction forces, frictional torque, distributed load and other parameters. During analysis of the interaction between elements in system "Vehicle – Track", these assumptions and conditions are considered:

- Rail deformation in X , Z directions;
- Interaction between roadbed and rail, as an elastic foundation;
- Possible gap between the sleeper and roadbed;
- Length of wheel and rail contact and geometrical unevenness appearing on it;
- The effect of rail axial forces on rigidity (due to differences in temperature);
- Initial bending of the rails;
- Possible gap between rail and sleeper;
- Bending of rail that is between two sleepers;
- Interaction of soil layers, that is under two adjacent sleepers;
- Wheel profile with damages;
- Contact zone is examined as linear contact according to X coordinate.

The system "Vehicle – Track" is examined in vertical direction. The computational scheme and its elements are shown in Figure 4.

Vehicle in computational model of system "Vehicle – Track" consists of (Appendix B and Fig. 4): 1/8 wagon mass m_{bg4} , 1/4 bogie mass m_{bg3} , 1/2 wheelset mass. Wheelset mass is divided into two parts: m_{bg1} - wheel mass, in direct contact with the rail and m_{bg2} - main wheelset mass.

During interaction between the wheel and the rail, the use of the wheel mass m_{bg1} a, which is directly in a contact with the rail, allows a more accurate assessment of the forces occurring on the wheel-rail contact and the kinematic parameters of the individual wheelset.

Track in computational model of system "Vehicle – Track" consists of (Fig. 4): rail (m_r), sleeper (m_{sl}) and railway roadbed m_{sl} . Roadbed consists of three layers (Appendix C): ballast (m_{s3}), sub-ballast (m_{s2}) and soil (m_{s1}).

Linear (marked as ovals in Fig. 4 and non-linear (marked as triangles in Fig. 4 stiffness and damping elements are used in the systems "Vehicle – Track".

2.3. Nonlinear dynamical computational algorithm for movement equations of system "Vehicle – Track"

System of movement equations of "Vehicle – Track" with the metal scale of wheelset wheel is equal to:

$$[M]\{\ddot{q}\} + [C]\{\dot{q}\} + [K]\{q\} = \{F_{NL}(q, \dot{q})\} + \{F(t)\} \quad (14)$$

where $[M]$, $[C]$, $[K]$, $\{F_{NL}(q, \dot{q}, t)\}$, $\{F(t)\}$ are mass, damping and stiffness matrices, nonlinear generalized force vector and external force vector, respectively. $\{q\}$, $\{\dot{q}\}$, $\{\ddot{q}\}$ are the system generalized displacements, velocities and accelerations vectors, respectively.

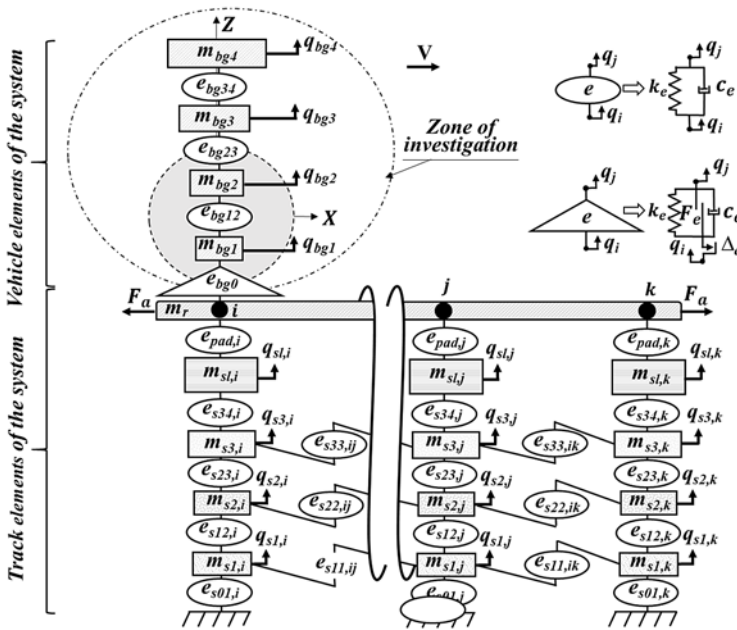


Fig. 4. Computational model of element interaction of system "Vehicle - Track"

Nonlinear generalized force $\{F_{NL}(q, \dot{q}, t)\}$ is extracted in the Taylor series at the point $\{q_k\}$:

$$\{F_{NL}(q, \dot{q})\} = \{F_{NL,k}\} + [K_{T,k}]\{\Delta q_k\} + [C_{T,k}]\{\Delta \dot{q}_k\}, \quad (15)$$

where: $[K_{T,k}] = \left[\frac{\partial \{F_{NL}(q_k, \dot{q}_k)\}}{\partial \{q\}} \right]$; $[C_{T,k}] = \left[\frac{\partial \{F_{NL}(q_k, \dot{q}_k)\}}{\partial \{\dot{q}\}} \right]$; $\{\Delta q_k\}$ and $\{\Delta \dot{q}_k\}$ are increments displacements and velocities vectors, respectively.

Then, the total system of equations (14), at the moment of time $t + \Delta t$, is equal to:

$$[M]\{\ddot{q}_{t+\Delta t}\} + [C]\{\dot{q}_{t+\Delta t}\} + [K]\{q_{t+\Delta t}\} - [C_T]\{\Delta \dot{q}_{t+\Delta t,k}\} - [K_T]\{\Delta q_{t+\Delta t,k}\} = \{F_{NL}(q_{t+\Delta t}, \dot{q}_{t+\Delta t})\} + \{F(t)\} \quad (16)$$

where Δt is integration time step; t is time.

By applying Newmark and Newton-Raphson methods, the total system for linear algebraic equations is solved in each of k -th iteration:

$$[A_{t+\Delta t,k}]\{\Delta q_k\} = -\{P_{t+\Delta t,k}\}, \text{ or } \{\Phi_{t+\Delta t,k}\} = [A_{t+\Delta t,k}]\{\Delta q_k\} + \{P_{t+\Delta t,k}\} = 0, \quad (17)$$

where:

$$[A_{t+\Delta t,k}] = \left(\frac{1}{\beta \Delta t^2} [M] + \frac{\gamma}{\beta \Delta t} ([C] - [C_{T,k}]) + ([K] - [K_{T,k}]) \right)$$

$$\{P_{t+\Delta t,k}\} = [M]\{\ddot{q}_{t+\Delta t,k}\} + [C]\{\dot{q}_{t+\Delta t,k}\} + [K]\{q_{t+\Delta t,k}\} - \{F_{NL,k}\} - \{F(t+\Delta t)\},$$

where: β, γ are the Newmark coefficients ($\gamma = 1/2, \beta = 1/4$).

The computational algorithm of nonlinear system "Vehicle - Track" is presented in Fig. 5.

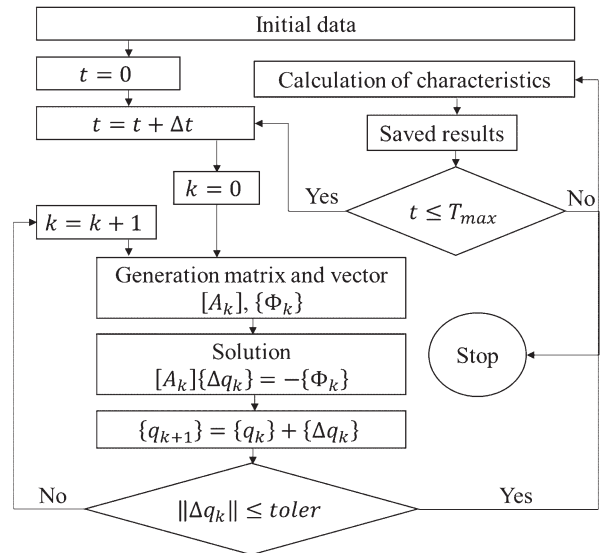


Fig. 5. Dynamical, nonlinear movement equation solving algorithm of system "Vehicle - Track"

An iterative process is performed in each time step, until the accuracy of solution is reached. Furthermore, the rate of displacement vector $\{\Delta q_k\}$ must be lower than the entered accuracy $\{\Delta q_k\} \leq toler$. Parameters of ballast, rail, wheel and the contact between them, speed, accelerations and other parameters must be saved at each time step.

Each of the computational parameters, given in the mathematical model, are averaged depending on the length of the wheel-rail contact. The computational process continues until the condition of $t \leq T_{max}$ is true. Such a solution is suitable for examination of system "Vehicle - Track", when the wheel is scaled, because the created wheelset scale model is three-dimensional.

3. Results and discussion

3.1. Initial data of research of the system "Vehicle - Track", when the wheel has a metal scale

The purpose of the research is to determine the interaction between wheel and rail, show how the wheel and rail movement changes and introduce the impact of geometrical parameters of metal scale on the dynamical loads occurring during the wheel-rail contact, by using the mathematical model of the system "Vehicle - Track", when the wheel has a metal scale. The system "Vehicle - Track" is analysed, when the vehicle wheel has radius $R_W = 0.495$ m and has a metal scale, is moving on the rail (R-65) at different speeds ($V = 40, 60, 80$,

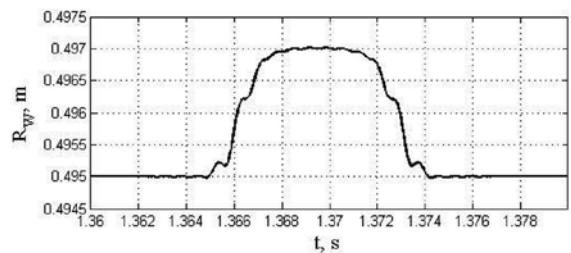


Fig. 6. Alteration of wheel radius, when the wagon is moving at speed $V = 40$ km/h, metal scale width $L_P = 100$ and at different heights of metal scale $h_{max} = 2$ mm, at time interval from 1.36 s to 1.38 s

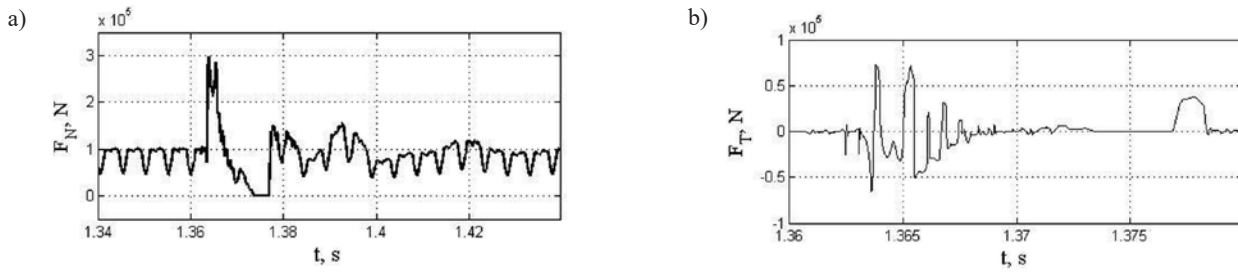


Fig. 7. Dependency of dynamic characteristics on time, when height of vehicle wheel scale is 2 mm and when the vehicle is moving at the speed of 40 km/h: a) normal force F_N at time interval from 1.34 s to 1.44 s; b) friction force F_T at time interval from 1.36 s to 1.38 s

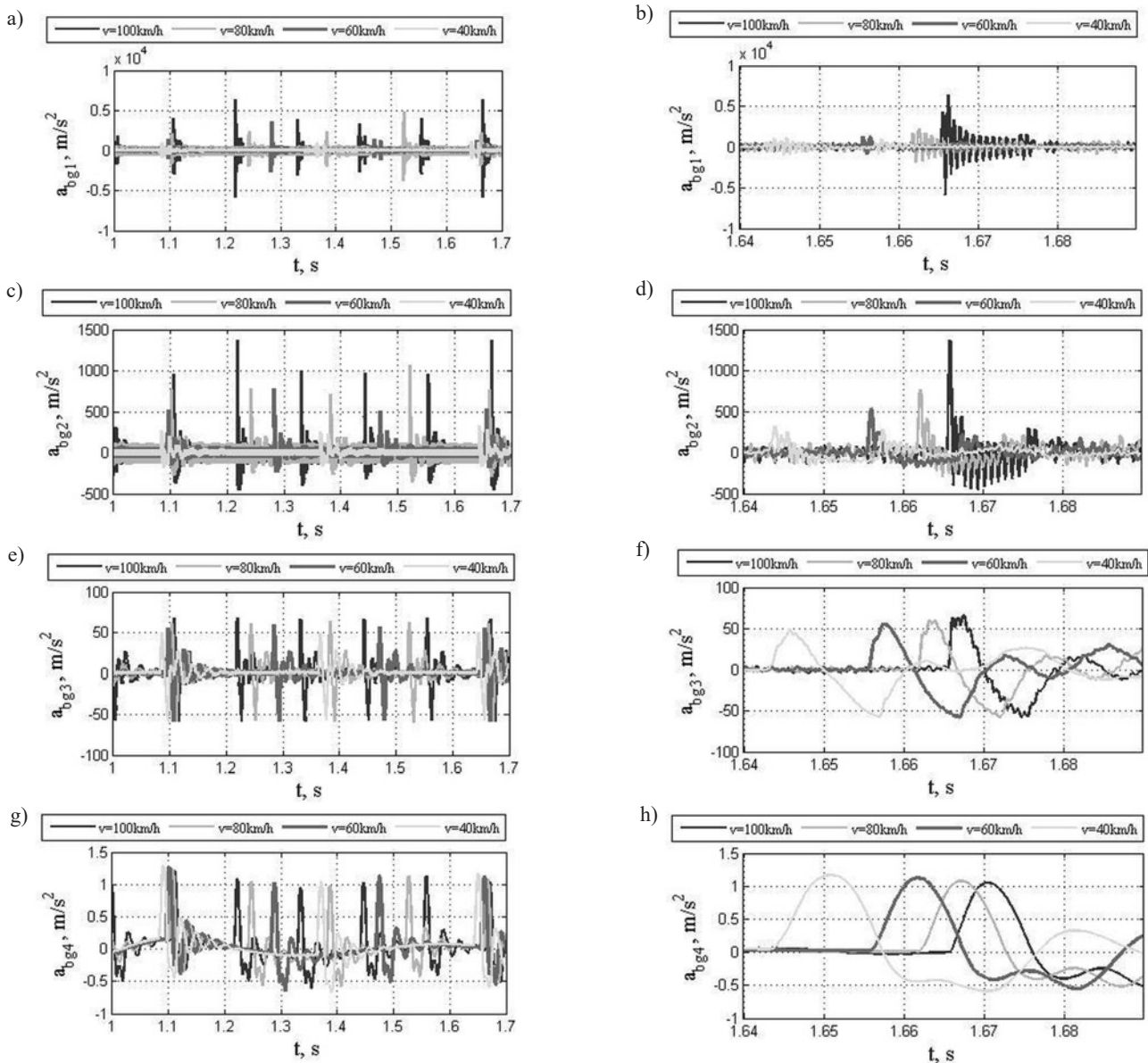


Fig. 8. Dependency of vehicle mass accelerations a_{bgi} on time, when the wheel is moving at different speeds and the wheel has a metal scale, which height is $h_{max} = 2$ mm: a) m_{bg1} in time interval from 1.0 s to 1.7 s; b) m_{bg1} in time interval from 1.635 s to 1.69 s; c) m_{bg2} in time interval from 1.0 s to 1.7 s; d) m_{bg2} in time interval from 1.635 s to 1.69 s; e) m_{bg3} in time interval from 1.0 s to 1.7 s; f) m_{bg3} in time interval from 1.635 s to 1.69 s; g) m_{bg4} in time interval from 1.0 s to 1.7 s; h) m_{bg4} in time interval from 1.635 s to 1.69 s

100 km/h), when the length of scale is $L = 100$ mm and the maximum height of scale is $h_{max} = 2$ mm.

The data of system “Vehicle – Track”, used in the calculations is published in previous author’s works [5, 27] and shown in Appen-

dix A. Integration time step is $\Delta t = 5 \cdot 10^{-6}$ s. A profile of a vehicle with scaled wheel is described using Fourier transformation, number of harmonics is $NH = 401$. The calculations assume, that average value of friction coefficient is $\mu = 0.135$, obtained from experiments

carried out by the authors [5, 31]. Friction coefficient between the vehicle wheels in relation to the rail must not be lesser than 0.09 - 0.12, otherwise a wheel slip may occur, due to its sticking.

3.2. Results and discussion of research of the system "Vehicle – Track", when the wheel has a metal scale

Dynamical characteristics of the wheel may alter due to damages in vehicle wheel. The developed model [5], allows a detailed analysis of kinematical and dynamical characteristics of system "Vehicle – Track". All parameters of calculations that are shown below are averaged according to the length of the contact.

The dependence of vehicle wheel radius R_W on time and height of metal scale of the wheel, when the movement speed is $V = 40$ km/h, is shown in Figure 6.

Wheel sliding on the deformed rail causes friction forces in contact zone. Dependency of normal forces F_N , friction forces F_T around the wheel longitudinal axis Y and on time, when vehicle wheel has $h_{max} = 2$ mm metal scales height and the vehicle is moving at the speed of 40 km/h, are shown in Figure 7.

Normal force F_N increases in the contact zone of wheel with metal scale and rail, when the metal scale is in the contact zone.

The value of this force depends on the size of the metal scale (Fig. 7 a) and the movement speed. When the movement speed of wheel is $V = 40$ km/h and the maximum height of metal scale is $h_{max} = 2$ mm, the maximum normal force F_N is equal to 300 kN.

Therefore, due to the wheel slip that appears in the contact zone (Fig. 8) and the normal force F_N acting in the contact, the friction force F_T must appear.

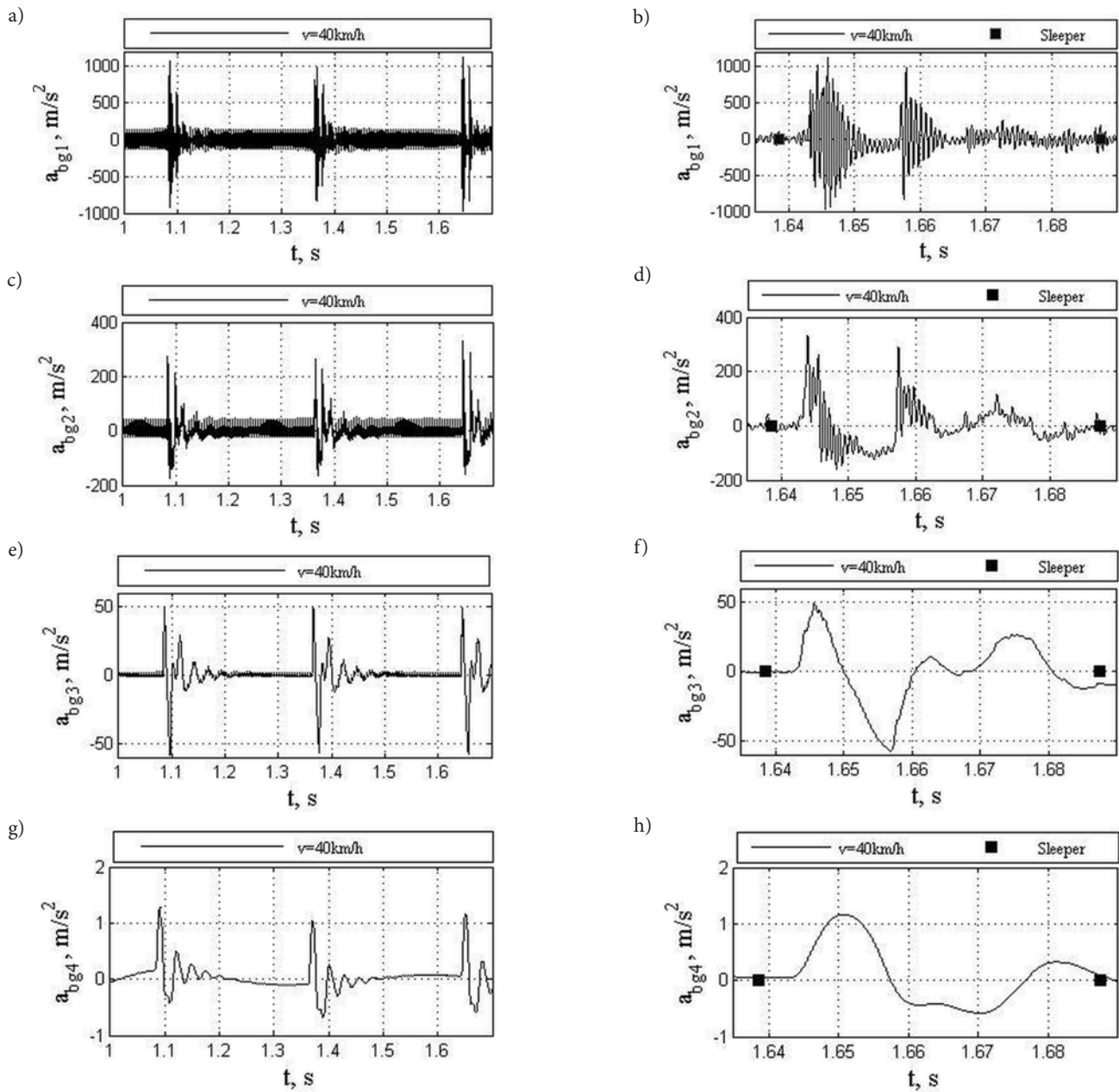


Fig. 9. Vehicle mass acceleration dependency a_{bgi} on time, when the wheel is with a metal scale (when $h_{max} = 2$ mm) moving at speed of 40 km/h: a) m_{bg1} in time interval from 1.0 s to 1.7 s; b) m_{bg1} in time interval from 1.635 s to 1.69 s; c) m_{bg2} in time interval from 1.0 s to 1.7 s; d) m_{bg2} in time interval from 1.635 to 1.69 s; e) m_{bg3} in time interval from 1.0 s to 1.7 s; f) m_{bg3} in time interval from 1.635 s to 1.69 s; g) m_{bg4} in time interval from 1.0 s to 1.7 s; h) m_{bg4} in time interval from 1.635 s to 1.69 s

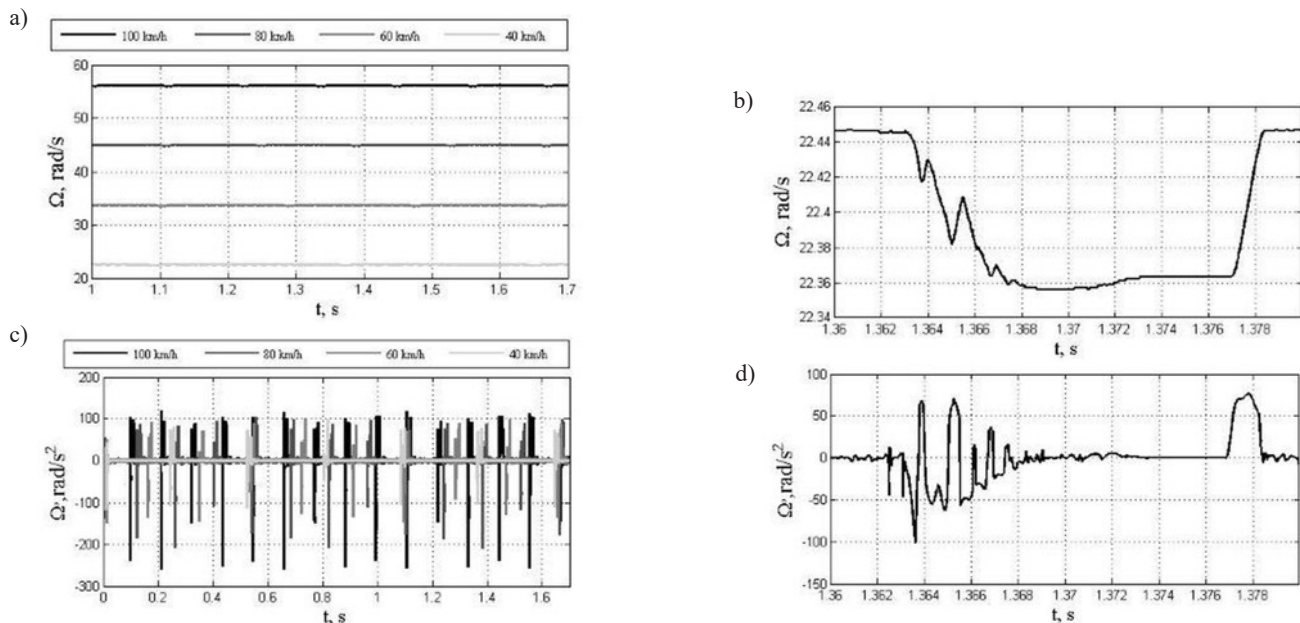


Fig. 10. Dependencies of the angular velocity of wheel Ω and angular acceleration $\ddot{\Omega}$ on time, when the vehicle wheel has a metal scale, with heights ($h_{max} = 2\text{ mm}$): a) angular velocity of wheel Ω , when vehicle is moving at different speeds ($V = 40, 60, 80, 100\text{ km/h}$), at time interval from 1.0 s to 1.7 s; b) angular velocity of wheel Ω at time interval from 1.36 s to 1.38 s, when the vehicle moves at speed of 40 km/h; c) wheel angular acceleration $\ddot{\Omega}$, when vehicle is moving at different speeds ($V = 40, 60, 80, 100\text{ km/h}$), at time interval from 1.0 s to 1.7 s; d) wheel angular acceleration $\ddot{\Omega}$ at time interval from 1.36 s to 1.38 s, when the vehicle moves at speed of 40 km/h

In Figure 8 it can be seen that acceleration of wheel (mass m_{bg2}) depends on the movement speed of the wheel. When the movement speed V changes (40 km/h, 60 km/h, 80 km/h, 100 km/h), the maximum acceleration of the wheel a_{bg2} alters to 350 m/s², 510 m/s², 750 m/s², 1400 m/s² and the minimum acceleration alters to 80 m/s², 150 m/s², 250 m/s², 490 m/s², respectively.

Parameters of interaction between wheel with metal scale and rail are dependent on contact zone of the rail. The closer the contact zone is to the sleeper, the bigger the rail stiffness and parameters of interaction are.

The vehicle mass m_{bgi} (when $i = 1, 2$) acceleration a_{bgi} dependencies on time and contact zone, when vehicle moves at speed $V = 40\text{ km/h}$ and wheel is with metal scale, which's height is $h_{max} = 2\text{ mm}$ are shown in Figure 9.

After a comparison of mass m_{bgi} accelerations (when $i = 1, 2$) a_{bgi} in time $t = 0.08\text{ s}$, 1.37 s, 1.66 s, it can be seen that, contact between wheel and rail is closer to sleeper at time $t = 1.66\text{ s}$. Wheel mass accelerations acquire highest values at this time. Contact between wheel and rail is most distant from the sleeper at time $t = 1.37\text{ s}$ and has the smallest mass acceleration. Dependency of vehicle mass m_{bgi} accelerations a_{bgi} (when $i = 1, 2$) on time, when vehicle wheel has a metal scale, which height is $h_{max} = 2\text{ mm}$ and the vehicle movement speed is $V = 40\text{ km/h}$.

Variations in time of the angular velocity of wheel Ω and angular acceleration $\ddot{\Omega}$, when the vehicle wheel has a metal scale, which height is $h_{max} = 2\text{ mm}$, at different moving speeds are shown in Figure 10 a, c and moving at speed $V = 40\text{ km/h}$ are shown in Figure 10 b, d.

In Figure 10, it can be seen that average angular velocity Ω and acceleration $\ddot{\Omega}$ of wheel with a metal scale decreases in the contact zone and its decrease depends on the movement speed.

Loads on sleepers of forces occurring in the contact zone of wheel with metal scale and rails, on sleeper when wheel movement speed is $V = 40\text{ km/h}$ and metal scale ($h_{max} = 2\text{ mm}$), are shown in Figure 11.

In Figure 11, it is possible to see, that the impact on rail occurs between sleepers 44 and 45, at the time 1.637 s. The impact force F_{pad} on rail loads up in to four sleepers in both directions from the most loaded sleeper (sleeper 45). Maximum force to sleepers, when wheel movement speed is $V = 40\text{ km/h}$ and the height of metal scale is ($h_{max} = 2\text{ mm}$), is equal to $F_{pad} = 130\text{ kN}$.

A more detailed method of interaction between the wheel with metal scale and rail has been developed, which allows determination of the forces and moments of the contact zone of wheel with a metal scale and rail. In most cases, scientists are investigating the problems of interaction between wheel with flat and rail, but in these studies, wheel geometry is simplified, resulting in a wide range of research results. Comprehensive studies of the forces acting on the contact of the wheel with metal scale and the rail contact area are not known to the authors of this article, which suggests that these studies are expanding the knowledge in this field.

The results obtained in this research determine the forces acting in the contact more accurately, as it details the geometry of wheel with metal scale and rail and the forces acting in their contact that arise due to the movement of the rail and wheel in relation to each other. The length of the contact area is divided into many elements (over 1000, element length is less than 0.100 mm), in whose points velocities and accelerations, slip speeds, friction forces and moments are determined at each time moment. A mathematical model of the system "Vehicle - Track" has been developed, which allows determination of the pressure distribution in the contact between wheel and rail, at any time moment.

Wheel's position on rail can be described in position phases. The first is the phase of landing, and the second is the phase of rising (Fig. 12). The first point of phase is on the rail, in the centre of the sleeper and the second one is in the middle of the rail that is located between two sleepers.

Vehicle wheel's impact force is distributed almost symmetrically from the contact zone to the right and left sides (Fig. 11), if the impact occurs between two sleepers, in the centre of the rail, i.e. at the second point of first phase. At the first point of the first phase, the pressure is

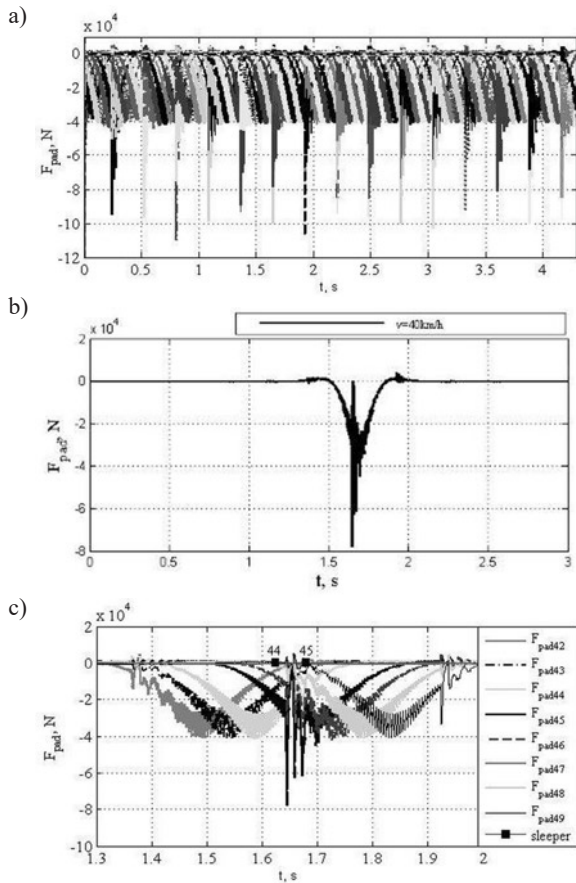


Fig. 11. Loads on sleepers of forces occurring in the contact zone of wheel with metal scale and rails, on sleeper when metal scale is $h_{max} = 2$ mm and wheel movement speed is $V = 40$ km/h

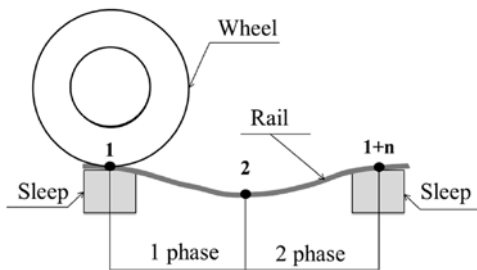


Fig. 12. Position phases of vehicle wheel

the highest. At the second phase, the friction forces increase, the soil and rail become deformed, when the wheel movement resistance is greater and that increases the weariness of wheel and rail. The developed mathematical model of the system „Vehicle – Track“ allows to determine the mass reduction of vehicle wheel with metal scale and rail, i.e. the weariness of profile of wheel with metal scale and rail.

Due to interaction between the wheel with the metal scale and the rail, at their points of contact increased forces and moments that overload the wheelset wheel and the rail appear. The values of these forces depend on the geometrical parameters of wheel, metal scale and rail, the movement speed of the wagon, the physical and mechanical properties of the roadbed, the dynamic characteristics of the wagon bogie, and the load on the wheelset wheel. The appearance of a metal scale on the wheel’s surface causes technical and operational problems for the rolling stock. Railway standards limit the speed of movement for a certain size of metal scale.

The results of this work confirm the statement that a wheelset wheel with a metal scale increases the load on the wheelset, the axle

box bearings, the rail, and reduces the durability and safe movement of the wheelset wheel and the rail. The developed method and obtained results of the research give a deeper insight into the problems of the wheel with metal scale and rail, as well as the analysis of the forces and moments involved in the contact, depending on the parameters of the system “Vehicle – Track” and the movement speed of the vehicle.

The developed method allows determination of the forces and moments occurring in the contact between wheel with metal scale and rail. It also allows to adjust the loads on wheel bearings, the permissible wagon speed, depending on the geometry of the wheel with metal scale, and determine the heat release in the contact, the speed and size of the wheel and rail wear, the reduction in ride comfort, etc. By using this method, it is possible to create monitoring systems for damaged wheels with metal scales.

The symmetrical profile of vehicle wheel changes during exploitation, due to changes in its radius. This mathematical method allows examining the changes in the wheel profile, if a flat, metal scale, other damages, or if other bodies appear on the surface of the wheel.

The main drawback of this research is that the zone of railway wheel with metal scale and rail is examined as a contact line, but the geometrical model of the metal scale is three-dimensional. The object of the research is the system „Vehicle-Track“, so the main focus was on description of contact geometry of rail and wheel with metal scale and on determination of contact forces and moments occurring in the contact zone. Research of interaction between surfaces of wheel and rail are provided later.

The release of heat is studied in the presence of wheel and rail interactions at contact points, the weariness of contacting bodies is studied with and without lubricants (fluid), and also the effect of the rail and wheel wheels on the friction forces and the wearing of the bodies are studied in the research. The increasing speeds of the railway transport show the importance of the problem of contact between the wheel with scale and the rail.

To ensure effective maintenance loads handing over to rail, forces that influence the rail are needed to establish. This method and research results can be used to calculate the interaction between track and other transport vehicles with solid (metal) wheels that have metal scale.

4. Conclusion

The developed spatial mathematical model of wheel with a metal scale (2-13) allows to divide the vehicle wheel surface perimeter into three zones during the generation of scaled wheel profile, also it is used to generate the shape of metal scale and if the geometry of scale is known – to generate the wheel profile with a metal scale.

The mathematical model allows evaluation of the wheel rotation around its longitudinal axis Y, in order to evaluate the rotation of the vehicle wheel and determine its slip on the rails.

It is determined, that when the height of metal scale is $h_{max} = 2$ mm and the length of scale is $L = 100$ mm, the maximum normal contact forces F_N is 300 kN, when the speed of moving wheelset alters $V = 40$ km/h, static wheel load is 100 kN and average wheel radius is $R_W = 0.495$ m.

When there is a metal scale on the wheel, which has a height of that $h_{max} = 2$ mm and length of $L = 100$ mm, the slipping of wheel on rail increases, maximum slipping speed alters from 0.0437 m/s ($V = 40$ km/h). Wheel slipping on rail causes friction forces in the contact, which increase the weariness of wheel and rail. The friction force in the contact F_T is 75 kN ($h_{max} = 2$ mm, $V = 40$ km/h). Part of mechanical power is converted to heat per unit of time, due to that, the temperature of wheel scale gets higher and the metal scale can be heavily worn.

Rail is loaded with short-term distributed load in the contact zone of wheel with metal scale and rail. The deforming rail transfers this load to the sleepers. It is determined, that the load on the wheel-rail contact zone loads up to four sleepers, when the distance between sleepers is 0.54 m.

The distributed load that acts on the contact zone of wheel with metal scale and rail, loads the wheel, therefore kinematical parameters of wheel, bogie and wagon alter. Because of metal scale that has formed in vehicle wheel, maximum acceleration of wheel is 336 m/s^2 ($h_{max} = 2 \text{ mm}$, $V = 40 \text{ km/h}$), maximum acceleration of bogie is 50 m/s^2 and maximum acceleration of wagon alter is 1.3 m/s^2 . The wheelset with scaled wheel not only increases wheelset wheel loads, but also increases loads of bogie, wagon and the wagon's cargo.

The method allows examination of dynamical processes occurring in the system „Vehicle – Track“, when the wheel is with a metal scale and the rail profiles are constantly changing.

It has been established, that the developed mathematical models of system “Vehicle – Track” and wheel is with a metal scale allow determination of the resistance forces between rail and wheel and determination of the energy loss, electricity and fuel consumptions. All of this is very important for the operation of the railway rolling stock, rail and road constructions.

Acknowledgement

This work has been supported by the European Social Fund within the project “Development and application of innovative research methods and solutions for traffic structures, vehicles and their flows”, project code VPI-3.1-ŠMM-08-K-01-020.

References

1. Bian J, Gu Y, Murray M H. A dynamic wheel-rail impact analysis of railway track under wheel flat by finite element analysis. *Vehicle System Dynamics* 2013; 1(6): 784-797, <https://doi.org/10.1080/00423114.2013.774031>.
2. Bogdevicius M, Zygiene R, Dailydka S, Bartulis V, Skrickij V, Pukalskas S. The dynamic behaviour of a wheel flat of a railway vehicle and rail irregularities. *Transport* 2015; 30(2): 217-232, <https://doi.org/10.3846/16484142.2015.1051108>.
3. Bogdevicius M, Zygiene R, Skrickij V, Methodology for the determination of maximum contact vertical wheel loads. *Transbaltica 2015: Proceedings of the 9th International Scientific Conference, May 7–8, 2015. Vilnius Gediminas Technical University, 2016; 134: 348-352*, <https://doi.org/10.1016/j.proeng.2016.01.018>.
4. Bogdevicius M, Zygiene R. Simulation dynamic processes of rail vehicle and rail with irregularities. *Journal KONES*. 2014; 21(2): 48-51, <https://doi.org/10.5604/12314005.1133858>.
5. Bogdevicius M., Zygiene R., Bureika G., Dailydka S. An analytical mathematical method for calculation of the dynamic wheel-rail impact force caused by wheel flat. *Vehicle System Dynamics* 2016; 54(5): 689-705, <https://doi.org/10.1080/00423114.2016.1153114>.
6. Bureika G, Bekintis G, Liudvinavičius L, Vaičiūnas G. Applying analytic hierarchy process to assess traffic safety risk of railway infrastructure. *Eksploatacja i Niezawodność – Maintenance and Reliability* 2013; 15(4): 376-383.
7. Chudzikiewicz A, Bogacz R St, Kostrzewski M, Konowrocki R. Condition Monitoring of Railway Track Systems by Using Acceleration Signals on Wheelset Axle-Boxes. *Transport* 2018; 33(2): 30-42, <https://doi.org/10.3846/16484142.2017.1342101>.
8. Domin R, Domin I, Cherniak G. Estimation of dynamic performances of the safe operation of highspeed electric train. *Archives of Transport* 2017; 41(1): 7-16, <https://doi.org/10.5604/01.3001.0009.7374>.
9. Ferrara R, Leonardi G, Jourdan F. Numerical Modelling of Train Induced Vibrations. *Procedia– Social and Behavioral Sciences (Sciencedirect)* 2012; 53: 155-165. <https://doi.org/10.1016/j.sbspro.2012.09.869>
10. Jazykov VI. Primenenie modeli negercevsogo kontakta koleasa s relsom dlia ocenki dinamicheskix kachestv gruzovogo teplovoza. *Dissertacija na soiskaniye stepeni kandidata technicheskix nauk*. Briansk: BG TU, 2004. (in Russian).
11. Keropyan A M. Determination of Rational Values of the Coefficients of Friction and Roughness of the Surfaces of Rails and Ties Locomotives. *Nedelia gorniaka*, 2014.
12. Keršys R, Bazaras Ž, Griškevičius P. Vagono vertikalios dinamikos modeliavimas. *Transport engineering* 1999; 5: 40-42.
13. Konop J, Konowrocki R. On Evaluation of the Wheelsets-Track Interaction Quality in Railway Engineering. *Machine Dynamics Research* 2013; 37(4): 61-70.
14. Kostrzewski M. Analysis of selected vibroacoustic signals recorded on EMU vehicle running on chosen routes under supervised operating conditions JVE International LTD. *Vibroengineering Procedia*. Sep. 2017; 13: 2345-0533, <https://doi.org/10.21595/vp.2017.18958>.
15. Kouroussis G, Gazetas G, Anastasopoulos I, Conti C, Verlinden O. Discrete modelling of vertical track-soil coupling for vehicle-track dynamics. *Soil Dynamics and Earthquake Engineering* 2011; 31(12): 1711-1723, <https://doi.org/10.1016/j.soildyn.2011.07.007>.
16. Kumar V, Rastogi V. Investigation of vertical dynamic behaviour and modelling of a typical Indian rail road vehicle through bond graph. *World Journal of Modelling and Simulation* 2009; 5(2): 130-138.
17. Nielsen J C O. High-frequency vertical wheel-rail contact forces – Validation of a prediction model by field testing. *Wear* 2008; 265: 1465-1471, <https://doi.org/10.1016/j.wear.2008.02.038>.
18. Nielsen J, Igeland A. Vertical dynamic interaction between train and track influence of wheel and track imperfections. *Journal of Sound and Vibration* 1995; 187(5): 825-839, <https://doi.org/10.1006/jsvi.1995.0566>.
19. Pieringer A, Kropp W, Nielsen J C O. The influence of contact modelling on simulated wheel/rail interaction due to wheel flats. *Wear* 2014; 314(1-2): 273-281, <https://doi.org/10.1016/j.wear.2013.12.005>.
20. Sackfield A, Dini D, Hills D A. Contact of a rotating wheel with a flat. *International Journal of Solids and Structures* 2007; 44(10): 3304-3316, <https://doi.org/10.1016/j.ijsolstr.2006.09.025>.
21. Sackfield A, Dini D, Hills D A. The contact problem for a wheel having a 'flat'. *Wear* 2006; 261(11-12): 1265-1270, <https://doi.org/10.1016/j.wear.2006.03.009>.
22. Shabana A A, Rathod C. Geometric coupling in the wheel/rail contact formulations: a comparative study. *Journal of Multi-body Dynamics* 2007; 221(2): 147-160, <https://doi.org/10.1243/14644193JMBD103>.
23. Shabana A A, El-Ghandour A I, Zaazaa K E. Study of the effect of the spiral geometry on wheel/rail contact forces. *Journal of Multi-body Dynamics* 2011; 225(2): 111-125, <https://doi.org/10.1177/1464419311406626>.

24. Sivilevičius H, Maskeliūnaitė L. The numerical example for evaluating the criteria describing the quality of the trip by international. E&M Economics and Management 2014; 2: 73-86, <https://doi.org/10.15240/tul/001/2014-2-006>.
25. Sladkowski A, Sitarz M. Analysis of wheel–rail interaction using FE software. Wear 2005; 258(7–8), 1217-1223, <https://doi.org/10.1016/j.wear.2004.03.032>.
26. TNN. Techninio geležinkelių naudojimo nuostatai. Lietuvos Respublikos susisiekimo ministro 1996 m. rugšėjo 20 d. įsakymas Nr. 297.
27. Turskis Z, Zavadskas E K. A new fuzzy additive ratio assessment method (ARAS-F). Case study: The analysis of fuzzy multiple criteria in order to select the logistic centers location. Transport 2010; 25: 423-432, <https://doi.org/10.3846/transport.2010.52>.
28. Vasauskas V, Bazaras Ž, Čapas V. Strength anisotropy of railway wheels under contact load. Mechanika 2005; 1(51): 31-38.
29. Wang K, Liu P F, Zhai W, Huang Ch, Chen Z, Gao J. Wheel/rail dynamic interaction due to excitation of rail corrugation in high-speed railway. Special Topic: High-speed Railway Infrastructure 2015; 58(2): 226-235, <https://doi.org/10.1007/s11431-014-5633-y>.
30. Wasiwitono U, Zheng D, Chiu W K. How useful is track acceleration for monitoring impact loads generated by wheel defects? In Proc. of the 5th Australasian Congress on Applied Mechanics, ACAM 2007, 10–12 December 2007, Brisbane, Australia, 2007: 502-507.
31. Zygiene R, Bogdevicius M, Dabuleviciene L. A mathematical model and simulation results of the dynamic system railway vehicle wheel–track with a wheel flat. Science – The future of Lithuania: Transport engineering, 2014; 6(5): 95-101, <https://doi.org/10.3846/mla.2014.696>.

Appendix A

Table A1. Data calculations of the system "Vehicle-Track"

Definition	Notation	Definition	Notation
Masses of ballast:	$m_{s1} = 800$ kg	Rail mass per meter	$m_R = 65$ kg/m
	$m_{s2} = 465$ kg	Static load	$F_x = 100$ kN
	$m_{s3} = 200$ kg	1/8 car body mass	$m_{bg4} = 8743$ kg
Damping coefficients of ballast:	$c_{s01} = 90$ kNs/m	1/4 bogie mass	$m_{bg3} = 700$ kg
	$c_{s12} = 70$ kNs/m	1/2 wheel set mass	$m_{bg2} = 640$ kg
	$c_{s23} = 60$ kNs/m	Mass in contact	$m_{bg1} = 110$ kg
	$c_{s34} = 50$ kNs/m	Stiffness coefficient of the car body	$k_{bg34} = 2.55$ MN/m
	$c_{s11,i,j} = 10$ kNs/m	Stiffness coefficient of the bogie	$k_{bg23} = 6.5$ MN/m
	$c_{s22,i,j} = 13$ kNs/m	Stiffness coefficient of the wheel set	$k_{bg12} = 5$ GN/m
	$c_{s33,i,j} = 15$ kNs/m	Damping coefficient of the car body	$c_{bg4} = 10$ kNs/m
	$k_{s01} = 180$ MN/m	Damping coefficient of the bogie	$c_{bg3} = 100$ kNs/m
	$k_{s12} = 170$ MN/m	Damping coefficient of the wheel set	$c_{bg2} = 50$ kNs/m
	$k_{s23} = 160$ MN/m	Damping coefficient of mass in contact	$c_{bg1} = 44.2$ kNs/m
Stiffness coefficients of ballast:	$k_{s34} = 150$ MN/m	Wheel radius	$R_W = 0.495$ m
	$k_{s11,i,j} = 15$ MN/m	Elastic modulus of the wheel	$E_W = 210$ GPa
	$k_{s22,i,j} = 16$ MN/m	Exponent	$n = 3 / 2$
	$k_{s33,i,j} = 17$ MN/m	Maximal penetration velocity	$\dot{\delta}_{max} = 10$ m/s
	Spacing between the sleepers centres	$L_{sl} = 0.5435$ m	Mass inertia moment of wheelset
Mass of the sleeper	$m_{sl} = 140$ kg	Restitution coefficient	$e = 0.65$
Width of a railway sleeper	$b_{sl} = 0.15$ m	Poisson's coefficient of the wheel	$\nu_W = 0.30$
Height of a railway sleeper	$h_{sl} = 0.12$ m	Friction parameters:	$\mu_{X0} = 0.14$
Number of finite elements between two sleepers	10		$\mu_X = 0.11$
Pad damping coefficient	$c_{pad} = 45$ kNs/m		$\gamma_v = -2.50$ s / m
Pad stiffness coefficient	$k_{pad} = 140$ MN/m		$k_s = 800$ s / m
The Second moment of the area of the rail about Z axis	$J_{RZ} = 5.69 \cdot 10^{-6}$ m ⁴	Contact length of wheel with rail	$L_{contact} = 100$ mm
The Second moment of the area of the rail about Y axis	$J_{RY} = 3.54 \cdot 10^{-5}$ m ⁴	Length of metal scale	$2b_{p1} = L_p = 0.1$ m
Elastic modulus of the rail	$E_R = 206$ GPa	Maximum heights of metal scale	$h_{max1} = 0.001$ m

Poisson's coefficient of the rail	$\nu_R = 0.30$	$h_{max2} = 0,003$ m
Cross-sectional area of the rail	$A_R = 82.9 \cdot 10^{-4}$ m ²	$h_{max3} = 0,005$ m
Rail density	$\rho_R = 7850$ kg/m ³	

Marijonas BOGDEVICIUS

Department of Mobile Machinery and Railway Transport
Vilnius Gediminas Technical University
Plytines g. 27, 10105 Vilnius, Lithuania

Rasa ZYGIENE

Department of study program of Electronics and Electrical
Engineering
Kaunas University of Applied Engineering Sciences,
Tvirtoves al. 35, 50155 Kaunas, Lithuania

E-mails: marijonas.bogdevicius@vgtu.lt, rasazz@gmail.com
